

The influence of nonlinear damping on the response of a piezoelectric cantilever sensor in a symmetric or asymmetric configuration

Giuseppe Habib^{1a}, Emanuel Fainshtein^{2b}, Kai-Dietrich Wolf^{3a} and Oded Gottlieb^{*2a}

¹ Department of Applied Mechanics, Budapest University of Technology and Economics, Budapest, Hungary

² Department of Mechanical Engineering, Technion - Israel Institute of Technology, Haifa, Israel

³ Institute for Security Systems, University of Wuppertal, Velbert, Germany

(Received May 13, 2022, Revised June 8, 2022, Accepted June 9, 2022)

Abstract. We investigate the influence of nonlinear viscoelastic damping on the response of a cantilever sensor covered by piezoelectric layers in a symmetric or asymmetric configuration. We formulate an initial-boundary-value problem which consistently incorporates both geometric and material nonlinearities including the effect of viscoelastic damping which cannot be ignored for micro- and nano-mechanical sensor operation in a vacuum environment. We employ an asymptotic multiple-scales methodology to yield the system nonlinear frequency response near its primary resonance and employ a model-based estimation procedure to deduce the system damping backbone curve from controlled experiments in vacuum. We discuss the effect of nonlinear damping on sensor applications for scanning probe microscopy.

Keywords: nonlinear viscoelastic damping; piezoelectric cantilever sensor; symmetric/asymmetric configuration

1. Introduction

Smart structural activation via piezoelectric patches or layers for identification and control of vibrations has been successful in a variety of applications (Sunar and Rao 1999, *et al.* 2009) that span both large scale energy harvesting (Betts *et al.* 2012, Roccia *et al.* 2020, Mishra *et al.* 2020) and microscale mass sensing (Kumar *et al.* 2011) or nanoscale imaging where the individual micro-cantilever sensors employed for atomic force microscopy (Wolf and Gottlieb 2002, Roeser *et al.* 2016) are fundamental elements of parallel scanning probe microscopy (Minne *et al.* 1999, Rangelow *et al.* 2007). We note that the accuracy of microscale imaging as well as control of cantilever vibration crucially depends on the quality of the mathematical model governing system response.

A successful implementation of mathematical models thus requires simultaneous solution of both elastodynamic and electrostatic boundary-value problems (Maugin 1985) which are typically solved by elaborate numerical methods (Tzou and Tzeng 1990). An alternative asymptotic singular perturbation approach for problems with a weak nonlinearity (Pai *et al.* 1998) has been verified experimentally for cantilever dynamics with both geometric nonlinearities (Zaretsky and da Silva 1994, Anderson *et al.* 1996, Tabaddor 2000, Zaitsev *et al.* 2012) and piezoelectric material nonlinearities (Usher and Sim 2005, Kumar *et al.* 2011). However, to our knowledge, the treatment of

viscoelastic damping (Poh *et al.* 1996) has been treated only numerically (Providakis *et al.* 2008, Kambali *et al.* 2019).

In this paper we formulate a nonlinear initial-boundary-value problem for a piezoelectric cantilever sensor operating near its primary resonance in a vacuum environment which consistently incorporates quadratic and cubic contributions for both geometric and piezoelectric material nonlinearities. We apply the asymptotic multiple-scales method to yield the slowly-varying evolution equations near primary resonance culminating with the system frequency response and employ a model-based estimation procedure to deduce the magnitude of nonlinear damping from controlled experiments in vacuum. We discuss the effect of nonlinear damping on sensor applications for scanning probe microscopy.

2. Problem formulation

The system examined, shown schematically in Fig. 1 is a cantilever beam covered by a single or two piezoelectric layers along its entire length. We extend the model derivation for a nonlinear piezoelectric cantilever proposed by Wolf and Gottlieb (2001, 2002) to incorporate the contribution of viscoelastic damping (Mora and Gottlieb 2017, Kambali *et al.* 2019) to yield the following field equation

$$\rho A v_{tt} = [\lambda v_x - H_{02}(v_x v_{xx}^2 + v_{xxx}) - H_{03}(v_{xx}^2)_x - H_{04}(v_{xx}^3)_x]_x - Q \quad (1)$$

Where ρA is the cantilever longitudinal mass density, H_{mn} are constant coefficients deduced from the electric enthalpy density per unit length for the symmetric or

*Corresponding author, Ph.D., Professor,

E-mail: oded@technion.ac.il

^a Professor, Ph.D.

^b Research Engineer, M.Sc.

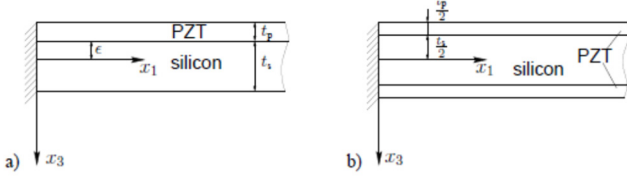


Fig. 1 Cantilever with piezoelectric layers:
(a) asymmetric; (b) symmetric configuration

asymmetric configurations (Wolf and Gottlieb 2001) and λ is the Lagrange multiplier required for implementation of the cantilever inextensibility condition to cubic order (Da Silva and Glynn 1978).

$$\lambda = \rho A \int_L^x u_{tt} dx - H_{02} v_x v_{xxx}, \quad u = -\frac{1}{2} \int_0^x v_x^2 dx \quad (2)$$

The viscoelastic force (Kambali *et al.* 2019) is

$$Q = Cv_t + DI[v_{xxxx}(1+v_x^2) + v_{xx}v_{xx}^2]_x \quad (3)$$

Where C is an equivalent viscous damping coefficient, D is a Kelvin-Voigt material damping parameter and I is the cantilever cross-section moment of inertia.

We rescale the field equation Eq. (1) via the cantilever length (L) and elastic time scale [$T = L^2(\rho A/H_{02})^{0.5}$] to yield the following nonlinear equation of motion

$$w_{\tau\tau} + (\bar{Q} + \bar{R} + \bar{S}) = 0 \quad (4)$$

Where \bar{Q} is the viscoelastic force which includes both linear and cubic components, \bar{R} is the restoring force which includes both linear and geometrically nonlinear cubic components and \bar{S} includes the contributions of both quadratic and cubic piezoelectric material components corresponding to the asymmetric and symmetric configurations respectively

$$\begin{aligned} \bar{Q} &= \mu_1 w_\tau + \mu_3 [w_{\tau s s s} (1 + w_s^2) + w_{\tau s} w_{s s}^2]_s \\ \bar{R} &= \left[w_{s s s} + w_s (w_s w_{s s})_s + \frac{w_s}{2} \int_1^\xi \frac{d^2}{d\tau^2} \left(\int_0^s w_s^2 ds \right) d\xi \right]_s \\ \bar{S} &= [\gamma_{32} (w_{s s}^2)_s + \gamma_{42} (w_{s s}^3)_s]_s \end{aligned} \quad (5)$$

Note that nondimensional field equation is governed by four nondimensional parameters $\mu_1 = (CT/\rho A)$, $\mu_3 = (D/ET)$, $\gamma_{32} = (H_{03}/LH_{02})$ and $\gamma_{42} = (H_{04}/L^2H_{02})$ where γ_{32} vanishes for the symmetric configuration. In anticipation of the weakly nonlinear asymptotic analysis we consider here only the linear contributions for the boundary conditions (Wolf and Gottlieb 2001) or $w(0, \tau) = w_s(0, \tau) = 0$, $w_{s s s}(1, \tau) = 0$ and $w_{s s}(1, \tau) = -\gamma_{12} \Delta \phi$ where $\gamma_{12} = (LH_{11}/H_{02})$ and $\Delta \phi = U \cos(\Omega \tau)$. Thus, the nondimensional initial-boundary-value problem is governed by seven parameters ($\mu_1, \mu_3, \gamma_{12}, \gamma_{32}, \gamma_{42}, U, \Omega$).

3. Asymptotic analysis

We employ an asymptotic multiple-scales solution procedure applied directly to the field equation and its

corresponding boundary conditions (Nayfeh 1981). Thus, the displacement is expanded into a power series

$$w(s, T_0, T_1, T_2) = \sum_{n=1}^3 \varepsilon^n w_n(s, T_0, T_1, T_2) \quad (6)$$

Where T_n are the time scales ($T_n = \varepsilon^n \tau$).

We substitute the assumed displacement in Eq. (6) and its derivatives into the equation of motion Eq. (4) and equate like coefficients of ε to yield the following sets of three PDEs and their corresponding boundary conditions

$$\begin{aligned} D_0^2 w_1 + w_{1 s s s s} &= 0, \\ w_1(0) = w_{1 s}(0) = w_{1 s s}(1) = w_{1 s s s}(1) &= 0, \\ D_0^2 w_2 + w_{2 s s s s} &= -2D_0 D_1 w_1 - \gamma_{32} (w_{1 s s}^2)_{s s}, \\ w_2(0) = w_{2 s}(0) = w_{2 s s}(1) = w_{2 s s s}(1) &= 0, \\ D_0^2 w_3 + w_{3 s s s s} &= -2D_0 D_1 w_2 - (D_1^2 + 2D_0 D_1 w_1) w_1 \\ &\quad - [(2\gamma_{32} (w_{1 s s} w_{2 s s})_{s s} + \gamma_{42} (w_{1 s s}^3)_{s s}) + (\bar{R} - w_{1 s s s s}) + \bar{S}], \\ w_3(0) = w_{3 s}(0) = w_{3 s s s}(1) &= 0, \\ w_{3 s s}(1) &= -\gamma_{12} U_3(T_0). \end{aligned} \quad (7)$$

Where $D_n = \partial/\partial T_n$ and we have defined sufficiently small viscous damping ($\mu_1 = \varepsilon^2 \bar{\mu}_1$) and small boundary amplitude excitation ($\Delta f = \varepsilon^3 U_3$) so that they appear in the third order set.

Solution of the first order set in Eq. (7) yields a standard linear solution for a Euler-Bernoulli beam. However, in order to prevent growth without bound for the second order set in Eq. (7) we impose a solvability condition ($D_1 A_1 = 0$) which enables solution of the non-secular particular solution of the second set (see details in Wolf and Gottlieb 2001). Substitution of the solutions w_1 and the non-secular w_2 from the first and second order sets respectively into the third order set in Eq. (7) requires an additional solvability condition to prevent solution growth without bound (Nayfeh 1981). This condition results in a slowly varying ($T_2 = \varepsilon^2 \tau$) complex amplitude evolution equation (Wolf and Gottlieb 2001) which in turn can be transformed to its autonomous form [$A_1(T_2) = a_1(T_2) \exp(i(\sigma T_2 - \theta_1(T_2)))$] where we have defined a small detuning (σ) from primary resonance [$\varepsilon^2 \sigma = (\Omega - \omega_1)$].

$$\begin{aligned} D_2 a_1 &= - \left(\frac{\bar{\mu}_1}{2} + \frac{3\mu_3}{8} a_1^2 \right) a_1 - \left(\frac{\alpha_{12} \gamma_{12} U_3}{2\omega_1} \right) \sin(\theta_1) \\ a_1 D_2 \theta_1 &= \left(\sigma - \frac{\gamma_C}{\omega_1} a_1^2 \right) a_1 - \left(\frac{\alpha_{12} \gamma_{12} U_3}{2\omega_1} \right) \cos(\theta_1) \end{aligned} \quad (8)$$

Where the effective cubic stiffness coefficient γ_C is a function of both the quadratic γ_{32} and cubic γ_{42} piezoelectric coefficients

$$\gamma_C = \left(\frac{3}{8} \alpha_1 - \frac{1}{2} \alpha_2 \omega_1^2 - \frac{1}{4} \alpha_{32} \gamma_{32}^2 + \frac{9}{8} \alpha_{42} \gamma_{42} \right) \quad (9)$$

And α_{ij} are integral coefficients which are a function of the primary resonance mode shape (see details in Wolf and Gottlieb 2001). Note that the contribution of the quadratic piezoelectric coefficient (γ_{32}) is always softening, whereas the cubic coefficient (γ_{42}) can be hardening or softening

(Nayfeh and Mook 1979).

The amplitude frequency response can readily be obtained from Eq. (8) by setting the slowly varying derivatives to zero so that the amplitude is solved for the detuning

$$\sigma = \left(\frac{\gamma_c}{\omega_1}\right) a_1^2 \pm \frac{1}{2} \sqrt{\left(\frac{v\gamma_f}{\omega_1 a_1}\right)^2 - \left(\bar{\mu}_1^2 + \frac{3}{8}\mu_3\omega_1^2 a_1^2\right)} \quad (10)$$

Where $v = \bar{U}_3/U_{\max}$ and $\gamma_f = \alpha_{12}\gamma_{12}U_{\max}$. We note that the amplitude frequency response in Eq. (10) reduces identically to the response without viscoelastic damping for both symmetric and asymmetric configurations (Wolf and Gottlieb 2001, 2002).

4. Model-based parameter estimation

We apply the asymptotic analysis to results obtained from a controlled set of experiments in a vacuum chamber to determine the frequency response amplitude from the slowly varying evolution formulation in Eq. (10). Fig. 2 depicts the layout and an enlargement and an enlargement of the piezo-cantilever (details in Fainshtein 2005).

An example set of measured amplitude frequency response functions (details in Habib 2008) are portrayed in Fig. 3 where we have varied the periodic input voltage (2.5-30.5 V).

We deduce and depict in Fig. 4 the damping backbone curve from the controlled experiments from both free vibration decay (Gottlieb and Habib 2012, Habib *et al.*

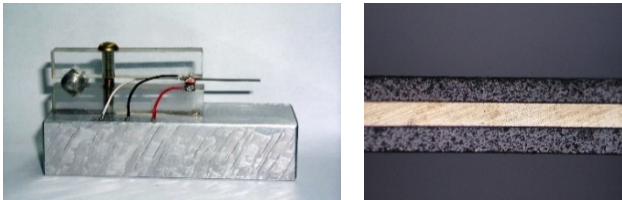


Fig. 2 The experiment layout and piezoelectric cantilever (Fainshtein 2005)

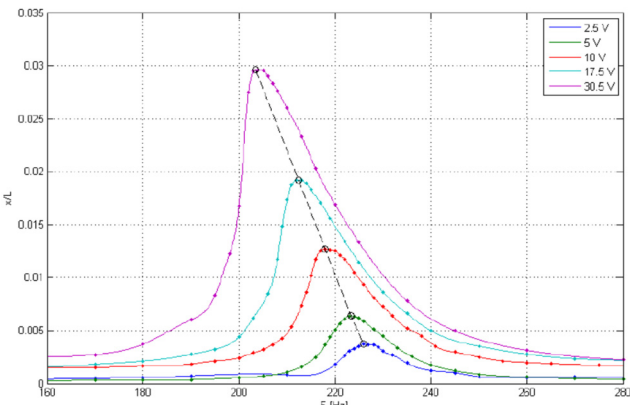


Fig. 3 The amplitude frequency response in vacuum obtained for several input voltages (2.5-30.5 Volts)

2017) and forced vibration due to periodic input excitation (Gottlieb *et al.* 1996). Thus, the equivalent damping ratio ζ can be obtained (Gottlieb and Habib 2012) from the slowly varying amplitude equation Eq. (8)

$$\zeta = \frac{1}{2}\mu_1 + \frac{3}{8}\mu_3(\omega_1 A)^2 \quad (11)$$

We note that the linear damping coefficient is proportional to the intersection of the damping ratio with the zero amplitude ($\mu_1 = 2\zeta$) whereas the nonlinear viscoelastic damping coefficient is proportional to the ratio between the equivalent damping and the amplitude squared [$\mu_3 = 4(2\zeta - \mu_1)/3(\omega_1 A)^2$].

5. Application to scanning probe microscopy

We extend the model-based estimation procedure to investigate scanning probe microscopy applications. For example, consider the case of magnetic force microscopy (Zuger and Rugar 1994, Kazakova *et al.* 2017, Vokoun *et al.* 2022) where a micro-cantilever with a magnetic tip is used to visualize magnetic fields from the surface of a ferromagnetic sample. This scanning probe microscopy methodology has been extended to detect changes in electron spin via magnetic resonance force microscopy (Rugar *et al.* 2004, Berman *et al.* 2006). The latter has revealed a complex internal resonance bifurcation structure (Hacker and Gottlieb 2017, 2020) and an expected increase of sensitivity in electron spin detection with matching frequencies of cantilever and spin (Berman and Tsifrinovich 2022).

We thus augment our piezoelectric cantilever experiment with a tip magnet and repeat the experiments in vacuum used for model-based estimation of the viscoelastic damping. Fig. 5. We note that the fundamental softening frequency response has remained softening. However, due to the magnetic interaction the resonance frequencies decreased by 15% (from the experiments with 2.5V the frequency of ~ 230 Hz in Fig. 3 to ~ 195 Hz in Fig. 5).

The corresponding backbone curve in Fig. 6 of the experiments depicted in Fig. 5 demonstrate that the magnitude of the linear damping coefficient obtained from

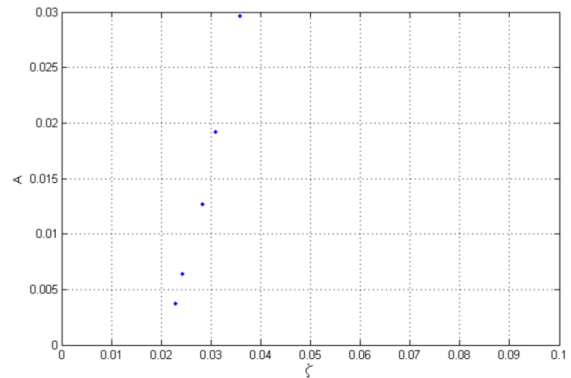


Fig. 4 The damping backbone curve corresponding to data in Fig.2 for a cantilever in vacuum

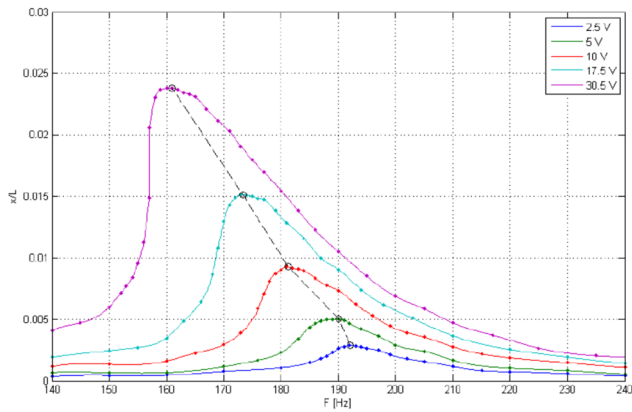


Fig. 5 The amplitude frequency response in vacuum of a cantilever with magnetic tip interaction obtained for several input voltages (2.5-30.5 Volts)

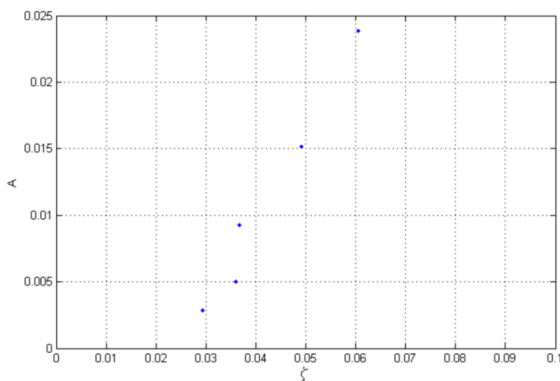


Fig. 6 The damping backbone curve corresponding to data in Fig. 5 for a cantilever in vacuum with magnetic tip interaction

the intersection of the backbone with the zero amplitude increased slightly ($\zeta \sim 0.023$) in comparison with the magnitude of linear damping without the magnetic interaction. However, the cubic viscoelastic coefficient did not change significantly.

6. Conclusions

A consistent nonlinear model for the dynamics of a piezoelectric cantilever with viscoelastic damping was derived. This model accounts for finite deformation and nonlinear behavior of both piezoelectric layers and viscoelastic material. For the geometry of a micro cantilever probe typical for scanning probe microscopy, the amplitude response to voltage excitation and its dependence on nonlinear damping has been determined by the asymptotic multiple-scales method near the dynamical system primary resonance. Model-based estimation of parameters from experiments of a vibrating cantilever in vacuum reveal a distinct softening behavior governed by the nonlinear properties of the piezoelectric material and the significance of non-negligible nonlinear damping of the constrained viscoelastic material.

Acknowledgments

The research described in this paper was supported in part by the Israel Science Foundation (Grant no. 136/16). O.G. was partially supported by the Henri Garik Chair in Mechanical Engineering. E.F. and K.W. acknowledge the support of their Technion graduate studies and postdoctoral fellowships, respectively.

References

- Anderson, T.A., Nayfeh, A.H. and Balachandran, B. (1996), "Experimental verification of the importance of nonlinear curvature in the response of a cantilever beam", *J. Vib. Acoust.* **118**(4), 21-27. <https://doi.org/10.1115/1.2889630>
- Betts, D.N., Kim, H.A., Bowen, C.R. and Inman, D.J. (2012), "Optimal configurations of bistable piezo-composites for energy harvesting", *Appl. Phys. Lett.*, **100**, 114104. <https://doi.org/10.1063/1.3693523>
- Berman, G.P. and Tsifrinovich, V.I. (2022), "Magnetic resonance force microscopy with matching frequencies of cantilever and spin", *J. Appl. Phys.*, **131**, 044301. <https://doi.org/10.1063/5.0073237>
- Berman, G.P., Borgonovi, F., Gorshkov, V.N. and Tsifrinovich, V.I. (2006), *Magnetic Resonance Force Microscopy and a Single-Spin Measurement*, World Scientific, Singapore.
- Da Silva, M.R.M.C. and Glynn, C.C. (1978), "Nonlinear flexural-torsional dynamics of inextensional beams – equations of motion", *J. Struct. Mech.*, **6**(4), 437-448. <https://doi.org/10.1080/03601217808907348>
- Fainshtein, E. (2005), "Nonlinear dynamics and stability of piezoelectric microbeams with application for atomic microscopy", M.Sc. Thesis; Technion - Israel Institute of Technology, Haifa, Israel.
- Gottlieb, O. and Habib, G. (2012), "Non-linear model-based estimation of quadratic and cubic damping mechanisms governing the dynamics of a chaotic spherical pendulum", *J. Vib. Control*, **18**(4), 536-547. <https://doi.org/10.1177/1077546310395969>
- Gottlieb, O., Feldman M. and Yim, S.C.S. (1996), "Parameter identification of nonlinear ocean mooring systems using the Hilbert transform", *J. Offshore Mech. And Arctic Eng.*, **118**, 29-36. <https://doi.org/10.1115/1.2828798>
- Habib, G. (2008), "Experimental analysis of linear and nonlinear vibrations of a piezoelectric cantilever in several conditions", M.Sc. Thesis; Sapienza University of Rome, Rome, Italy.
- Habib, G., Miklos, A., Enilov, E.T., Stepan, G. and Rega, G. (2017), "Nonlinear model-based parameter estimation and stability analysis of an aero-pendulum subject to digital delayed control", *Int. J. Dyn. Contr.*, **5**, 629-643. <https://doi.org/10.1007/s40435-015-0203-0>
- Hacker, E. and Gottlieb, O. (2017), "Application of reconstitution multiple scale asymptotics for a two-to-one internal resonance in Magnetic Resonance Force Microscopy", *Int. J. Nonlin. Mech.*, **94**, 174-199. <https://doi.org/10.1016/j.ijnonlinmec.2017.04.013>
- Hacker, E. and Gottlieb, O. (2020), "Local and global bifurcations in magnetic resonance force microscopy", *Int. J. Nonlin. Mech.*, **99**, 201-225. <https://doi.org/10.1007/s11071-019-05401-y>
- Kambali, P.N., Torres, F., Barniol, N. and Gottlieb, O. (2019), "Nonlinear multi-element interactions in an elastically coupled microcantilever array subject to electrodynamic excitation", *Nonlin. Dyn.*, **98**, 3067-3094. <https://doi.org/10.1007/s11071-019-05074-7>
- Kazakova, O., Puttock, R., Barton, C., Corte-León, H., Jaafar, M.,

- Neu, V. and Asenjo, A. (2017), "Frontiers of magnetic force microscopy", *J. Appl. Phys.* **125**, 060901.
<https://doi.org/10.1063/1.5050712>
- Kumar, V., Boley, J.W., Yang, Y., Ekowaluyo, H., Miller, J.K., Chiu, G.T.C. and Rhoads, J.F. (2011), "Bifurcation-based mass sensing using piezoelectrically-actuated microcantilevers", *Appl. Phys. Lett.*, **98**, 153510. <https://doi.org/10.1063/1.3574920>
- Manna, M.C., Sheikh, A.H. and Bhattacharyya, R. (2009), "Static analysis of rubber components with piezoelectric patches using nonlinear finite elements", *Smart Struct. Syst., Int. J.*, **5**(1), 23-42. <https://doi.org/10.12989/sss.2009.5.1.023>
- Maugin, G.A. (1985), *Nonlinear Electromechanical Effects and Applications*, World Scientific, Singapore.
- Minne, S., Manalis, S. and Quate, C. (1999), *Bringing Scanning Probe Microscopy up to Speed*, Springer Science & Business Media, Kluwer, Dordrecht, The Netherlands.
- Mishra K., Panda, S.K., Kumar, V. and Dewangan, H.C. (2020), "Analytical evaluation and experimental validation of energy harvesting using low-frequency band of piezoelectric bimorph actuator", *Smart Struct. Syst., Int. J.*, **26**(3), 391-401.
<https://doi.org/10.12989/sss.2020.26.3.391>
- Mora, K. and Gottlieb, O. (2017), "Parametric excitation of a microbeam-string with asymmetric electrodes: multimode dynamics and the effect of nonlinear damping", *J. Vib. Acoust.*, **139**, 040903. <https://doi.org/10.1115/1.4036632>
- Nayfeh, A.H. (1981), *Introduction to Perturbation Techniques*, Wiley, New York, USA.
- Nayfeh, A.H. and Mook, D.T. (1979), *Nonlinear Oscillations*, Wiley, New York, USA.
- Pai, P.B., Wen, A.N. and Schultz, M. (1998), "Structural vibration control using pzt patches and nonlinear phenomena", *J. Sound Vib.*, **215**, 273-296. <https://doi.org/10.1006/jsvi.1998.1612>
- Poh, S., Baz, A. and Balachandran, B. (1996), "Experimental adaptive control of sound radiation from a panel into an acoustic cavity using active constrained layer damping", *Smart Mater. Struct.*, **5**, 649-659. <https://doi.org/10.1088/0964-1726/5/5/013>
- Providakis, C.P., Kontoni, D.P.N., Voutetaki, M.E. and Stavroulaki, M.E. (2008), "Comparisons of smart damping treatments based on FEM modeling of electromechanical impedance", *Smart Struct. Syst., Int. J.*, **4**(1), 35-46.
<https://doi.org/10.12989/sss.2008.4.1.035>
- Rangelow, I.W., Ivanov, T., Ivanova, K., Volland, B.E., Grabiec, P., Sarov, Y., Persaud, A., Gotszalk, T., Zawierucha, P., Zielony, M. and Dontzov, D. (2007), "Piezoresistive and self-actuated 128-cantilever arrays for nanotechnology applications", *Microelect. Eng.*, **84**, 1260-1264. <https://doi.org/10.1016/j.mee.2007.01.219>
- Roccia, B.A., Verstaete, M.L., Ceballos, L.R., Balachandran, B. and Preidikman, S. (2020), "Computational study on aerodynamically coupled piezoelectric harvesters", *J. Intel. Mater. Sys.*, **31**(13), 1578-1593.
<https://doi.org/10.1177/1045389X20930093>
- Roeser, D., Gutschmidt, S., Sattel, T. and Rangelow, I.W. (2016), "Tip motion-sensor signal relation for a composite SPM/SPL cantilever", *J. Microelectromech. Syst.*, **25**(1), 78-90.
<https://doi.org/10.1109/JMEMS.2015.2482389>
- Rugar, D., Budakian, R., Mamin, H.J. and Chui, B.W. (2004), "Single spin detection by magnetic resonance force microscopy", *Nature*, **430**, 329-332.
<https://doi.org/10.1038/nature02658>
- Sunar, M. and Rao, S. (1999), "Recent advances in sensing and control of flexible structures via piezoelectric materials technology", *Appl. Mech. Rev.*, **52**(1) 1-16.
<https://doi.org/10.1115/1.3098923>
- Tabaddor, M. (2000), "Influence of nonlinear boundary conditions on the single-mode response of a cantilever beam", *Int. J. Solids Struct.*, **37**, 4915-4931.
[https://doi.org/10.1016/S0020-7683\(99\)00197-3](https://doi.org/10.1016/S0020-7683(99)00197-3)
- Tzou, H. and Tzeng, C. (1990), "Distributed piezoelectric sensor/actuation design for dynamic measurement control of distributed systems: a piezoelectric finite element approach", *J. Sound Vib.*, **138**(1), 17-34.
[https://doi.org/10.1016/0022-460X\(90\)90701-Z](https://doi.org/10.1016/0022-460X(90)90701-Z)
- Usher, T. and Sim, A. (2005), "Nonlinear dynamics of piezoelectric high displacement actuators in cantilever mode", *J. Appl. Phys.*, **98**, 064102, 1-7. <https://doi.org/10.1063/1.2041844>
- Vokoun, D., Samal, S. and Stachiv, I. (2022), "Magnetic force microscopy in physics and biomedical applications", *Magnetochemistry*, **8**(42), 1-14.
<https://doi.org/10.3390/magnetochemistry8040042>
- Wolf, K. and Gottlieb, O. (2001), "Nonlinear dynamics of a cantilever beam actuated by piezoelectric layers in symmetric and asymmetric configurations", Research Report No. ETR-2001-02, Technion-Israel Institute of Technology.
- Wolf, K. and Gottlieb, O. (2002), "Nonlinear dynamics of a non-contacting atomic force microscope cantilever actuated by a piezoelectric layer", *J. Appl. Phys.* **91**(7), 4701-4709.
<https://doi.org/10.1063/1.1458056>
- Zaitsev, S., Shtempluck, O., Buks, E. and Gottlieb, O. (2019), "Nonlinear damping in a micromechanical oscillator", *Nonlin. Dyn.*, **67**, 859-883. <https://doi.org/10.1007/s11071-011-0031-5>
- Zaretsky, C.L. and da Silva, M.R.M.C. (1994), "Experimental investigation of nonlinear modal coupling in the response of cantilever beams", *J. Sound Vib.*, **174**(2), 145-167.
<https://doi.org/10.1006/jsvi.1994.1268>
- Zuger, O. and Rugar, D. (1994), "Magnetic resonance detection and imaging using force microscope techniques", *J. Appl. Phys.*, **75**(10), 6211-6216. <https://doi.org/10.1063/1.355403>